Chem Biol Drug Des 2014; **83:** 297–305

Research Article

Synthesis and Evaluation of Novel Oleanolic Acid Derivatives as Potential Antidiabetic Agents

Liying Zhang[1], Xiaojian Jia[2], Jizhe Dong[3], Dongyin Chen[3], Jun Liu[4,*], Luyong Zhang[4] and Xiaoan Wen[3,*]

[1]Key Laboratory of Traditional Chinese Medicine Research and Development of Hebei Province, Institute of Traditional Chinese Medicine, Chengde Medical University, Chengde 067000, China
[2]School of Life Science & Technology, China Pharmaceutical University, Nanjing 21009, China
[3]Center for Drug Discovery, China Pharmaceutical University, Nanjing 21009, China
[4]Jiangsu Center for Drug Screening, China Pharmaceutical University, Nanjing 21009, China
**Corresponding authors: Jun Liu, junliu@cpu. edu.cn; Xiaoan Wen, wxagj@126.com*

Antidiabetic agents simultaneously inhibiting hepatic glucose production and stimulating hepatic glucose consumption could apply a better control over hyperglycemia. A series of oleanolic acid derivatives with bulky substituents at C-3 position were designed and synthesized in order to search for this kind of agents. All of the compounds were evaluated biologically *in vitro* using glycogen phosphorylase and HepG2 cells. The results indicated that several derivatives exhibited moderate-to-good inhibitory activities against glycogen phosphorylase. Compound 8g showed the best inhibition with an IC_{50} value of 5.4 μM. Moreover, most of the derivatives were found to increase the glucose consumption in HepG2 cells in a dose-dependent manner. The possible binding mode of compound 8g with glycogen phosphorylase was also explored by docking study. 8g was found to have hydrogen bonding interactions with Arg193, Arg310, and Arg60 of the allosteric site.

Key words: binding mode, glycogen phosphorylase inhibitors, hepatic glucose consumption, hepatic glucose production, oleanolic acid

Abbreviations: GP, glycogen phosphorylase; PEPCK, phosphoenolpyruvate carboxykinase; FBPase, fructose-1,6-bisphosphatase; G6Pase, glucose-6-phosphatase; GS, glycogen synthase; GK, glucokinase; 6PFK1, 6-phosphofructo-1-kinase; PK, pyruvate kinase; OA, oleanolic acid; HepG2, human hepatocellular carcinoma cell line; NMR, nuclear magnetic resonance; IR, infrared spectrometry; DMF, N, N-dimethylformamide; THF, tetrahydrofuran; Pd-C, palladium on carbon; DMSO, dimethyl sulfoxide; IC_{50}, half maximal inhibitory concentration; SD, standard deviation; RMGPa, rabbit muscle glycogen phosphorylase a; SAR, structure–activity relationship.

Received 21 June 2013, revised 28 August 2013 and accepted for publication 24 September 2013

The liver plays a dominant role in the regulation of glucose homeostasis because it is an organ of glucose production as well as glucose consumption. When blood glucose declines, the liver breaks down glycogen and releases glucose into the bloodstream. When plasma glucose levels are high, the liver takes up glucose, replenishes depleted glycogen stores, thus helping to dampen variations in blood glucose (1).

Type 2 diabetes is associated with the liver's inability to control glucose homeostasis (2). The defects of insulin to trigger downstream actions in liver are defined as hepatic insulin resistance, including increased hepatic glucose production and decreased hepatic glucose consumption (3). Therefore, in principle, any effect that decreases glucose production or increases glucose consumption, or both, would lead to a reduction in plasma glucose levels. From the perspective of enzymes involved in glucose metabolism, glycogen phosphorylase (GP), phosphoenolpyruvate carboxykinase (PEPCK), fructose-1,6-bisphosphatase (FBPase), and glucose-6-phosphatase (G6Pase) work together to generate glucose, whereas glycogen synthase (GS), glucokinase (GK), 6-phosphofructo-1-kinase (6PFK1), and pyruvate kinase (PK) work together for glucose disposal in the liver (4).

Oleanolic acid (**OA**, **1**), a pentacyclic triterpenoid compound isolated from the traditional Chinese herb *Ligustrum lucidum* Ait, exhibits a significant activity in lowering fasting blood glucose level (5). Unlike the commonly used antidiabetic therapeutics such as insulin or thiazolidinediones that up-regulate glucose transport in periphery and often lead to weight gain, **OA** possesses glucose-lowering activity, but lacks the adipogenic activity (6). Studies indicated that the liver may be the major site for the sustained improvement of glycemia after the treatment with **OA** (7). Previously, we have found that **OA** and its derivatives represented a novel class of inhibitors of GP (8), and their anti-hyperglycemia activity could, at least in part, be due to the modulation of hepatic glucose production. Recently, we first screened

 doi: 10.1111/cbdd.12241

the effect of **OA** on glucose consumption in human hepatocellular carcinoma cell line (HepG2) cells. **OA** significantly promoted the glucose consumption in HepG2 cells. Considering the hypoglycemic phenomenon, we postulated that the antidiabetic pharmacological effects of **OA** and its derivatives were not only due to the suppression of hepatic glucose production but also maybe partly due to the enhancement of hepatic glucose consumption.

Our previously reported data suggested that the proper substitutions at C-3 position conferred enhanced hypoglycemic activities (9). However, the C-3 ester groups of prior **OA** analogs have mainly contained freely rotating short alkyl chains. It is still unclear whether the increasing alkyl chain length or introducing aromatic substitutions is associated with increased hypoglycemic activities. Therefore, in the present study, a series of **OA** derivatives with long alkyl chains or aromatic rings at C-3 position were designed in order to further explore the conformational space of the C-3 pharmacophore. Furthermore, an attractive strategy for the linking conjugation involves the click reaction of azide-bearing **OA** with alkyne-bearing alkyl or aromatic groups to join them via a triazole linkage. The triazole linkage is more than just a passive linker because it readily associates with biological targets, through hydrogen bonding and dipole interactions (10).

In this article, we report our preliminary attempt to discover a novel of antidiabetic agents that inhibit hepatic glucose production and promote hepatic glucose consumption based on a simple and economical synthetic procedure (Figure 1). Biological evaluation of the derivatives as new GP inhibitors is also presented. Moreover, the glucose consumption was examined by measuring the glucose concentration in the medium after treatment with the synthesized compounds. To the best of our knowledge, no other dual-action compounds targeting both hepatic glucose production and hepatic glucose consumption have been reported.

Materials and Methods

Chemistry

Purifications by column chromatography were carried out over silica gel (200–400 mesh). Melting points were obtained on a MEL-TEMP II melting-point apparatus and are uncorrected. NMR spectra were recorded on a BRUKER-ACF-300 instrument (300 MHz for ^{1}H NMR and 75 MHz for ^{13}C NMR spectra, chemical shifts are expressed as values relative to TMS as internal standard). Mass spectral data were obtained on Agilent 1100 LC/DAD/MSD or Q-Tof Micro MS/MS. IR spectra were recorded on Shimadzu FTIR-8400S spectrometer. Compounds **4**–**6** were prepared according to the procedures as previously reported in the literature (9).

General procedure for the synthesis of 3a–3g

To a solution of carboxylic acid (**2a**–**2g**, 3.20 mmol) in DMF (10 mL) were added propargyl bromide (3.58 mmol) and K_2CO_3 (6.40 mmol). The reaction mixture was stirred at room temperature for 6–24 h and filtered. The filtrate was concentrated under vacuum, and the resultant residue was redissolved in ethyl acetate (50 mL). The organic layer was washed with 1 N HCl, saturated $NaHCO_3$, and brine and then dried (Na_2SO_4) and filtered. The filtrate was evaporated under vacuum to give a crude product alkyne-functionalized intermediate (**3a**–**3g**), which was used for the next reaction without further purification.

General procedure for the synthesis of 7a–7g

To a mixture of alkyne-functionalized intermediate (**3a**–**3g**, 0.48 mmol) and azide **6** (9) (0.48 mmol) in CH_2Cl_2 (1.5 mL) and H_2O (1.5 mL) were added $CuSO_4{\cdot}5H_2O$ (0.095 mmol) and sodium ascorbate (0.19 mmol). The resulting solution was stirred at room temperature for 2–8 h and filtered. The filtrate was concentrated under vacuum, and the resultant residue was redissolved in CH_2Cl_2 (5 mL). The reaction mixture was extracted with CH_2Cl_2 (3 × 5 mL). The combined organic layers were washed with brine, dried (Na_2SO_4), filtered, and concentrated. The residue was purified by flash column chromatography.

Benzyl 3β-[2-(4-nonanoyloxymethyl-1*H*-1,2,3-triazol-1-yl)acetoxy]olean-12-en-28-oate (7a)

White solid; yield: 91%; mp 63–65 °C. IR (KBr,per cm) ν 2948, 2856, 2106, 1732, 1464. ^{1}H-NMR ($CDCl_3$, 300 MHz) δ 0.63, 0.77, 0.86, 0.88, 0.91, 0.93, 0.95, 1.15 (s, each 3H), 2.34 (t, J = 7.5 Hz, 2H), 2.93 (dd, J = 3.9, 13.8 Hz, 1H), 4.58–4.63 (m, 1H), 5.07 (d, J = 12.6 Hz,

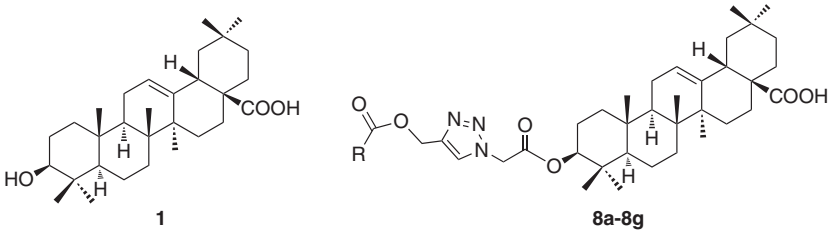

Figure 1: Structure of oleanolic acid (**OA**, **1**) and **OA** derivatives (**8a**–**8g**).

1H), 5.10 (d, *J* = 12.6 Hz, 1H), 5.18 (s, 2H), 5.27 (s, 2H), 5.31(br *s*, 1H), 7.29–7.36 (m, 5H), 7.77 (s, 1H). ^{13}C-NMR ($CDCl_3$, 75 MHz) δ 177.4, 173.7, 165.7, 143.8, 143.5, 136.4, 128.4, 127.9, 127.8, 125.1, 122.3, 83.9, 65.9, 57.3, 55.2, 51.1, 47.5, 46.7, 45.8, 41.6, 41.4, 39.2, 38.0, 34.1, 33.8, 33.1, 32.6, 32.3, 31.7, 30.6, 29.2, 29.1, 28.1, 27.5, 25.8, 24.8, 23.6, 23.4, 23.0, 22.6, 18.1, 16.8, 16.5, 15.3, 14.0. MS (ESI, m/z): 848.6 $[M+Na]^+$.

Benzyl 3β-[2-(4-decanoyloxymethyl-1*H*-1,2,3-triazol-1-yl)acetoxy]olean-12-en-28-oate (7b)

White solid; yield: 87%; mp 65–67 °C. IR (KBr, per cm) ν 3447, 2948, 2853, 1735, 1464. ^{1}H-NMR ($CDCl_3$, 300 MHz) δ 0.60, 0.73, 0.83, 0.89, 0.89, 0.91, 1.11, 1.25 (s, each 3H), 2.31 (t, *J* = 7.3 Hz, 2H), 2.89 (d, *J* = 9.7 Hz, 1H), 4.54–4.60 (m, 1H), 5.03 (d, *J* = 12.4 Hz, 1H), 5.09 (d, *J* = 12.4 Hz, 1H), 5.15 (s, 1H), 5.24 (s, 2H), 5.28 (br *s*, 1H), 7.32-7.35 (m, 5H), 7.73 (s, 1H). ^{13}C-NMR ($CDCl_3$, 75 MHz) δ 177.4, 173.7, 165.8, 143.8, 143.5, 136.4, 128.4, 128.0, 127.9, 125.1, 122.3, 83.9, 65.9, 57.4, 55.2, 51.1, 47.5, 46.7, 45.8, 41.7, 41.4, 39.3, 38.0, 37.7, 36.8, 34.1, 33.8, 32.6, 32.3, 31.9, 30.7, 29.4, 29.3, 29.1, 28.1, 27.6, 25.8, 24.8, 23.6, 23.4, 23.0, 22.7, 18.1, 16.8, 16.5, 15.3, 14.1. MS (ESI, m/z): 840.8 $[M+H]^+$.

Benzyl 3β-[2-(4-dodecanoyloxymethyl-1*H*-1,2,3-triazol-1-yl)acetoxy]olean-12-en-28-oate (7c)

White solid; yield: 81%; mp 66–68 °C. IR (KBr, per cm) ν 2926, 2853, 1735, 1465. ^{1}H-NMR ($CDCl_3$, 300 MHz) δ 0.60, 0.74, 0.83, 0.89, 0.91, 1.16, 1.24 (s, each 3H), 2.31 (t, 2H), 2.88 (dd, *J* = 4.1, 13.8 Hz, 1H), 4.54–4.60 (m, 1H), 5.03 (d, *J* = 12.5 Hz, 1H), 5.09 (d, *J* = 12.5 Hz, 1H), 5.14 (s, 2H), 5.23 (s, 2H), 5.27 (t, 1H, *J* = 3.0 Hz), 7.29–7.36 (m, 5H), 7.73 (s, 1H). ^{13}C-NMR ($CDCl_3$, 75 MHz) δ 177.3, 173.6, 165.7, 143.8, 143.5, 136.4, 128.4, 127.9, 127.8, 125.0, 122.3, 83.9, 65.9, 57.3, 55.2, 51.1, 47.5, 46.7, 45.9, 41.7, 41.4, 39.3, 38.0, 37.7, 36.9, 34.1, 33.9, 33.0, 32.6, 32.4, 31.9, 30.7, 29.6, 29.4, 29.3, 29.2, 29.1, 28.1, 27.6, 25.8, 24.8, 23.6, 23.4, 23.0, 22.6, 18.1, 16.9, 16.5, 15.3, 14.0. ESI-MS (ESI, m/z): 868.8 $[M+H]^+$.

Benzyl 3β-[2-(4-palmitoyloxymethyl-1*H*-1,2,3-triazol-1-yl)acetoxy]olean-12-en-28-oate (7d)

White solid; yield: 83%; mp 56–58 °C. IR (KBr, per cm) ν 2924, 2852, 1735, 1465. ^{1}H-NMR ($CDCl_3$, 300 MHz) δ 0.60, 0.73, 0.83, 0.85, 0.88, 0.89, 0.91, 1.11 (s, each 3H), 2.31 (t, *J* = 7.4 Hz, 2H), 2.91 (dd, *J* = 4.2, 13.8 Hz, 1H), 4.54–4.59 (m, 1H), 5.03 (d, *J* = 12.5 Hz, 1H), 5.09 (d, *J* = 12.5 Hz, 1H), 5.14 (s, 2H), 5.23 (s, 2H), 5.27(t, *J* = 3.4 Hz, 1H), 7.29–7.36 (m, 5H), 7.73 (s, 1H). ^{13}C-NMR ($CDCl_3$, 75 MHz) δ 177.3, 173.6, 165.7, 143.7, 143.5, 136.4, 128.4, 127.9, 125.0, 122.3, 83.9, 65.9, 57.3, 55.2, 51.1, 47.5, 46.7, 45.9, 41.7, 41.4, 39.3, 38.0, 37.7, 36.9, 34.1, 33.9, 33.0, 32.6, 32.4, 31.9, 30.7, 29.7, 29.6, 29.4, 29.3, 29.2, 29.1, 28.1, 27.6, 25.8, 24.8, 23.6, 23.4, 23.0, 22.6, 18.1, 16.9, 16.5, 15.3, 14.0. MS (ESI, m/z): 924.9 $[M+H]^+$.

Benzyl 3β-[2-(4-stearoyloxymethyl-1*H*-1,2,3-triazol-1-yl)acetoxy]olean-12-en-28-oate (7e)

White solid; yield: 89%; mp 50–52 °C. IR (KBr, per cm) ν 2924, 2852, 1737, 1464. ^{1}H-NMR ($CDCl_3$, 300 MHz) δ 0.60, 0.74, 0.83, 0.88, 0.89, 0.89, 0.91, 1.11 (s, each 3H), 2.31 (t, *J* = 7.7 Hz, 2H), 2.90 (dd, *J* = 4.2, 13.7 Hz, 1H), 4.54–4.60 (m, 1H), 5.02 (d, *J* = 12.6 Hz, 1H), 5.06 (d, *J* = 12.6 Hz, 1H), 5.14 (s, 2H), 5.23 (s, 2H), 5.27 (t, *J* = 3.6 Hz, 1H), 7.27–7.35 (m, 5H), 7.73 (s, 1H). ^{13}C-NMR ($CDCl_3$, 75 MHz) δ 177.4, 173.7, 165.7, 143.8, 143.5, 136.5, 128.4, 128.0, 127.9, 125.1, 122.3, 84.0, 65.9, 57.4, 55.3, 51.2, 47.6, 45.9, 46.7, 41.7, 41.4, 39.3, 38.0, 37.8, 36.9, 34.2, 33.9, 33.1, 32.6, 32.4, 31.9, 30.7, 29.7, 29.7, 29.6, 29.5, 29.3, 29.2, 29.1, 28.1, 27.6, 25.8, 24.8, 23.6, 23.4, 23.0, 22.6, 18.1, 16.9, 16.5, 15.3, 14.0. MS (ESI, m/z): 953.0 $[M+H]^+$.

Benzyl 3β-{2-[4-(4-methoxybenzoyloxy)methyl-1*H*-1,2,3-triazol-1-yl]acetoxy}olean-12-en-28-oate (7f)

White solid; yield: 91%; mp 89–91 °C. IR (KBr, per cm) ν 2948, 1720, 1606, 1511. ^{1}H-NMR ($CDCl_3$, 300 MHz) δ 0.58, 0.65, 0.78, 0.83, 0.89, 0.91, 1.20 (s, each 3H), 2.90 (dd, *J* = 3.5, 13.7 Hz, 1H), 3.86 (s, 3H), 4.52–4.57 (m, 1H), 5.03 (d, *J* = 12.6 Hz, 1H), 5.09 (d, *J* = 12.6 Hz, 1H), 5.16 (s, 2H), 5.28 (t, *J* = 3.8 Hz, 1H), 5.47 (br *s*, 2H), 6.89 (d, *J* = 8.8 Hz, 2H), 7.28–7.33 (m, 5H), 7.82 (br *s*, 1H), 7.98 (d, *J* = 8.8 Hz, 2H). ^{13}C-NMR ($CDCl_3$, 75 MHz) δ 177.4, 166.1, 165.7, 163.6, 143.7, 136.8, 131.8, 128.4, 128.0, 127.9, 122.3, 122.2, 113.6, 83.9, 65.9, 57.7, 55.4, 55.2, 51.2, 47.5, 46.7, 45.9, 41.6, 41.4, 39.2, 37.9, 37.7, 36.8, 33.8, 33.1, 32.6, 32.4, 30.7, 28.0, 27.6, 25.8, 23.6, 23.4, 23.0, 18.1, 16.8, 16.5, 15.2. MS (ESI, m/z): 842.5 $[M+Na]^+$.

Benzyl 3β-{2-[4-(2-naphthalen-2-yl)acetoxymethyl-1*H*-1,2,3-triazol-1-yl]acetoxy}olean-12-en-28-oate (7 g)

White solid; yield: 86%; mp 91–93 °C. IR (KBr, per cm) ν 2947, 2854, 1734, 1700. ^{1}H-NMR ($CDCl_3$, 300 MHz) δ 0.60, 0.72, 0.81, 0.88, 0.89, 0.92, 1.12 (s, each 3H), 2.89 (d, *J* = 10.0 Hz, 1H), 4.01 (s, 2H), 4.53–4.56 (m, 1H), 5.02–5.12 (m, 4H), 5.27 (br *s*, 3H), 7.33–7.53 (m, 9H), 7.78–7.94 (m, 3H). ^{13}C-NMR ($CDCl_3$, 75 MHz) δ 177.4, 165.7, 143.8, 143.2, 136.5, 128.7, 128.4, 128.2, 128.1, 128.0, 127.9, 126.4, 125.8, 125.5, 125.1, 123.8, 122.3, 83.9, 65.9, 58.1, 55.3, 51.1, 47.6, 46.8, 45.9, 41.7, 41.4, 39.3, 38.9, 38.0, 37.8, 36.9, 33.9, 33.1, 32.6, 32.4, 30.7, 28.1, 27.6, 25.8, 23.6, 23.4, 23.1, 18.2, 16.9, 16.5, 15.3. MS (ESI, m/z): 854.6 $[M+H]^+$.

General procedure for the synthesis of 8a-8 g

To a solution of benzyl ester (**7a**–**7g**, 0.35 mmol) in THF (5 mL) was added 10% Pd-C (0.3 g), with stirring under hydrogen atmosphere at room temperature for 12 h. The catalyst was filtered through Celite, and the filtrate was concentrated under vacuum to give a crude product that was purified by flash column chromatography.

3β-[2-(4-nonanoyloxymethyl-1*H*-1,2,3-triazol-1-yl) acetoxy]olean-12-en-28-oic acid (8a)

White solid; yield: 87%; mp 132–134 °C. IR (KBr, per cm) *ν* 2928, 1743, 1692, 1465. ^{1}H-NMR ($CDCl_3$, 300 MHz) *δ* 0.74 (s, 6H), 0.81, 0.84, 0.87, 0.90, 0.92, 1.12 (s, each 3H), 2.31 (t, *J* = 7.5 Hz, 2H), 2.82 (d, *J* = 9.9 Hz, 1H), 4.55–4.60 (m, 1H), 5.15 (s, 2H), 5.24 (s, 2H), 5.31 (br *s*, 1H), 7.74 (s, 1H). ^{13}C-NMR ($CDCl_3$, 75 MHz) *δ* 183.6, 165.8, 143.6, 143.4, 125.1, 122.4, 83.9, 57.3, 55.2, 51.1, 47.5, 46.5, 45.8, 41.6, 40.9, 39.2, 37.9, 37.7, 36.9, 34.1, 33.8, 33.0, 32.5, 31.8, 30.6, 29.2, 29.1, 28.1, 27.6, 25.9, 24.8, 23.5, 23.4, 22.9, 22.6, 18.1, 17.1, 16.5, 15.3, 14.1. MS (ESI, m/z): 734.7[*M*−H]$^-$. HR-MS (ESI, M+H) m/z: calcd for $C_{44}H_{70}N_3O_6$ 736.52591, found 736.52825.

3β-[2-(4-decanoyloxymethyl-1*H*-1,2,3-triazol-1-yl) acetoxy]olean-12-en-28-oic acid (8b)

White solid; yield: 88%; mp 160–162 °C. IR (KBr, per cm) *ν* 3382, 2925, 1741, 1691. ^{1}H-NMR ($CDCl_3$, 300 MHz) *δ* 0.75, 0.75, 0.84, 0.88, 0.90, 0.92, 0.92, 1.13 (s, each 3H), 2.31 (t, *J* = 7.4 Hz, 2H), 2.81 (d, *J* = 9.5 Hz, 1H), 4.56–4.61 (m, 1H), 5.16 (s, 2H), 5.24 (s, 2H), 5.28 (br *s*, 1H), 7.74 (s, 1H). ^{13}C-NMR ($CDCl_3$, 75 MHz) *δ* 183.7, 173.6, 165.7, 143.6, 143.4, 125.1, 122.3, 83.8, 57.3, 55.1, 51.0, 47.4, 46.4, 45.8, 41.5, 40.9, 39.2, 37.9, 37.7, 36.9, 34.1, 33.7, 33.0, 32.3, 31.8, 30.6, 29.3, 29.2, 29.0, 28.0, 27.6, 25.8, 24.8, 23.5, 23.3, 22.8, 22.6, 18.1, 17.0, 16.4, 15.3, 14.0. MS (ESI, m/z): 788.0 [*M*+K]$^+$. HR-MS (ESI, M-H) m/z: calcd for $C_{45}H_{70}N_3O_6$ 748.5265, found 748.5263.

3β-[2-(4-dodecanoyloxymethyl-1*H*-1,2,3-triazol-1-yl)acetoxy]olean-12-en-28-oic acid (8c)

White solid; yield: 79%; mp 163–164 °C. IR(KBr, per cm) *ν* 2928, 2852, 1740, 1693. ^{1}H-NMR ($CDCl_3$, 300 MHz) *δ* 0.75, 0.75, 0.84, 0.86, 0.88, 0.90, 0.92, 1.13 (s, each 3H), 2.31 (t, *J* = 7.4 Hz, 2H), 2.81 (d, *J* = 13.8 Hz, 1H), 4.55-4.61 (m, 1H), 5.16 (s, 2H), 5.24 (s, 2H), 5.28 (br *s*, 1H), 7.73 (s, 1H). ^{13}C-NMR ($CDCl_3$, 75 MHz) *δ* 183.6, 173.7, 165.8, 143.6, 143.4, 125.1, 122.4, 83.9, 57.3, 55.2, 51.1, 47.5, 46.5, 45.8, 41.6, 40.9, 39.2, 37.9, 37.7, 36.9, 34.1, 33.8, 33.0, 32.4, 31.9, 30.6, 29.6, 29.4, 29.3, 29.2, 29.1, 28.1, 27.6, 25.9, 24.8, 23.5, 23.4, 22.9, 22.7, 18.1, 17.1, 16.5, 15.3, 14.1. MS (ESI, m/z): 776.6 [*M*-H]$^-$. HR-MS (ESI, M-H) m/z: calcd for $C_{47}H_{74}N_3O_6$ 776.5578, found 776.5581.

3β-[2-(4-palmitoyloxymethyl-1*H*-1,2,3-triazol-1-yl) acetoxy]olean-12-en-28-oic acid (8d)

White solid; yield: 93%; mp 129–131 °C. IR(KBr, per cm) *ν* 2924, 2852, 1740, 1693, 1465. ^{1}H-NMR ($CDCl_3$, 300 MHz) *δ* 0.75, 0.75, 0.84, 0.86, 0.88, 0.90, 0.92, 1.13 (s, each 3H), 2.31 (t, *J* = 7.5 Hz, 2H), 2.82 (dd, *J* = 3.5, 13.5 Hz, 1H), 4.56–4.61 (m, 1H), 5.15 (s, 2H), 5.24 (s, 2H), 5.28 (br *s*, 1H), 7.74 (s, 1H). ^{13}C-NMR ($CDCl_3$, 75 MHz) *δ* 173.7, 165.8, 143.6, 143.5, 125.1, 122.4, 83.9, 57.3, 55.2, 51.1, 47.5, 46.5, 45.8, 41.6, 41.0, 39.3, 37.9, 37.7, 36.9, 34.1, 33.8, 33.0, 32.4, 31.9, 30.7, 29.7, 29.6, 29.4, 29.3, 29.2, 29.1, 28.1, 27.6, 25.9, 24.8, 23.6, 23.4, 22.9, 22.7, 18.1, 17.1, 16.5, 15.3, 14.1. MS (ESI, m/z): 832.5[*M*−H]$^-$. HR-MS (ESI, M-H) m/z: calcd for $C_{51}H_{82}N_3O_6$ 832.6204, found 832.6202.

3β-[2-(4-stearoyloxymethyl-1*H*-1,2,3-triazol-1-yl) acetoxy]olean-12-en-28-oic acid (8e)

White solid; yield: 90%; mp 149–150 °C. IR(KBr, per cm) *ν* 2923, 2850, 1741, 1693, 1466. ^{1}H-NMR ($CDCl_3$, 300 MHz) *δ* 0.74 (s, 6H), 0.81, 0.84, 0.88, 0.90, 0.92, 1.12 (s, each 3H), 2.31 (t, *J* = 7.4 Hz, 2H), 2.80 (dd, *J* = 2.4, 12.9 Hz, 1H), 4.55–4.60 (m, 1H), 5.15 (s, 2H), 5.24 (s, 2H), 5.27 (br *s*, 1H), 7.74 (s, 1H). ^{13}C-NMR ($CDCl_3$, 75 MHz) *δ* 182.8, 173.7, 165.8, 143.7, 143.5, 125.1, 122.4, 83.9, 57.4, 55.3, 51.2, 47.6, 46.5, 45.9, 41.7, 41.1, 39.3, 38.0, 37.8, 37.0, 34.2, 33.8, 33.0, 32.6, 32.5, 31.9, 30.7, 29.5, 29.3, 29.3, 29.1, 28.1, 27.7, 25.9, 24.9, 23.6, 23.4, 23.0, 22.7, 18.2, 17.1, 16.5, 15.3, 14.1. MS (ESI, m/z): 862.6[*M*+H]$^+$. HR-MS (ESI, M+Na) m/z: calcd for $C_{53}H_{87}N_3Na_1O_6$ 884.64871, found 884.64672.

3β-{2-[4-(4-methoxybenzoyloxy)methyl-1*H*-1,2,3-triazol-1-yl]acetoxy}olean-12-en-28-oic acid (8f)

White solid; yield: 75%; mp 174–175 °C. IR(KBr, per cm) *ν* 2946, 1745, 1712, 1694. ^{1}H-NMR ($CDCl_3$, 300 MHz) *δ* 0.67, 0.73, 0.80, 0.87, 0.90, 0.92, 1.12 (s, each 3H), 2.81 (dd, *J* = 3.8, 13.6 Hz, 1H), 3.84 (s, 3H), 4.53–4.58 (m, 1H), 5.16 (s, 2H), 5.26 (br *s*, 1H), 5.47 (s, 2H), 6.89 (d, *J* = 9.7 Hz, 2H), 7.83 (s, 1H), 7.99 (d, *J* = 9.7 Hz, 2H). ^{13}C-NMR ($CDCl_3$, 75 MHz) *δ* 165.7, 143.6, 131.8, 125.3, 122.4, 113.6, 83.8, 57.7, 55.4, 55.2, 51.2, 47.5, 46.5, 45.8, 41.6, 41.0, 39.3, 37.9, 37.7, 36.9, 33.8, 33.0, 32.5, 32.4, 30.6, 28.0, 27.6, 25.9, 23.6, 23.4, 22.9, 18.1, 17.0, 16.4, 15.3. MS (ESI, m/z): 728.4[*M*−H]$^-$. HR-MS (ESI, M+H) m/z: calcd for $C_{43}H_{60}N_3O_7$ 730.44258, found 730.44429.

3β-{2-[4-(2-naphthalen-1-yl)acetoxymethyl-1*H*-1,2,3-triazol-1-yl]acetoxy}olean-12-en-28-oic acid (8 g)

White solid; yield: 84%; mp 100–102 °C. IR(KBr, per cm) *ν* 2945, 2873, 1740, 1691. ^{1}H-NMR ($CDCl_3$, 300 MHz) *δ* 0.65, 0.69, 0.75, 0.84, 0.85, 0.86, 1.06 (s, each 3H), 2.75 (d, *J* = 10.2 Hz, 1H), 4.01 (s, 2H), 4.47–4.52 (m, 1H), 4.99

(s, 2H), 5.20 (s, 3H), 7.32–7.45 (m, 4H), 7.70–7.87 (m, 3H). ^{13}C-NMR ($CDCl_3$, 75 MHz): δ 183.0, 171.4, 165.7, 143.7, 143.2, 133.9, 132.1, 130.2, 128.7, 128.2, 128.1, 126.4, 125.8, 125.5, 125.1, 123.7, 122.4, 83.9, 58.1, 55.2, 51.1, 47.6, 46.5, 45.9, 41.6, 41.0, 39.3, 38.9, 38.0, 37.8, 37.0, 33.8, 33.0, 32.5, 32.5, 30.7, 28.1, 27.7, 25.9, 23.6, 23.4, 22.9, 18.2, 17.1, 16.5, 15.3. MS (ESI, m/z): 762.4 $[M-H]^-$. HR-MS (ESI, M-H) m/z: calcd for $C_{47}H_{60}N_3O_6$ 762.4482, found 762.4484.

Biological studies

Assay of glycogen phosphorylase inhibitory activity

The inhibitory activity of the synthesized compounds against rabbit muscle glycogen phosphorylase a (RMGPa) was monitored using microplate reader (BIO-RAD, Hercules, CA, USA) based on the published method (11). In brief, RMGPa activity was measured in the direction of glycogen synthesis by the release of phosphate from glucose-1-phosphate. Each test compound was dissolved in DMSO and diluted at different concentrations for IC_{50} determination. The enzyme was added into 100 μL of buffer containing 50 mM Hepes (pH = 7.2), 100 mM KCl, 2.5 mM $MgCl_2$, 0.5 mM glucose-1-phosphate, 1 mg/mL glycogen, and the test compound in 96-well microplates (Costar, Cambridge, MA, USA). After the addition of 150 μL of 1 M HCl containing 10 mg/mL ammonium molybdate and 0.38 mg/mL malachite green, reactions were run at 22 °C for 25 min, and then, the phosphate absorbance was measured at 655 nm. The IC_{50} values were estimated by fitting the inhibition data to a dose-dependent curve using a logistic derivative equation.

Measurement of the glucose consumption in HepG2 cells

HepG2 cells (ATCC, Manassas, VA, USA) were cultured in Gibco RPMI-1640 media (Invitrogen, Carlsbad, CA, USA) supplemented with 10% fetal bovine serum (Invitrogen), and maintained at 37 °C with 5% CO_2. The glucose concentration of RPMI-1640 is 11.11 mM. For screening, cells were plated into 96-well plates (Corning Incorporated, NY, USA) at a density of 1×10^5 cells/well in serum-containing medium. After 20 h, cells (80–90% confluence) were washed once and incubated in serum-free RPMI-1640 containing DMSO (0.1%), insulin (0.1 μM), and different doses of target compounds (1 and 10 μM). Changes in the glucose concentrations in aliquots from the culture media after HepG2 incubation for 24 h were determined by glucose oxidase–peroxidase method with a commercial diagnostic kit (Jiancheng Bioengineering Institute, Nanjing, China) (12). Results reported in all analyses were derived from at least three independent experiments. All values were presented as mean ± SD. Data are presented as mean values, and error bars indicate SD in chart. Student's *t*-test was used to determine the difference between control and treatment groups. One-way ANOVA followed by Dunnett's multiple comparison test was performed for multiple comparisons between the groups. Statistical significance was accepted at $p < 0.05$, indicated in Figure 3 as follows: *$p < 0.05$; **$p < 0.01$; ***$p < 0.001$.

Docking study

The docking analysis was performed using the sketch molecule module of Sybyl 6.9 package (Tripos Inc., St. Louis, MO, USA). The crystal structure of GP complexed with maslinic acid at the allosteric site was received from the Protein Data Bank (PDB code: 2QN2) (8). All the hydrogen atoms were added to specify the correct configuration and tautomeric states. Then, the modeled structure was energy-minimized using AMBER 7 F99 force field with distance-dependent dielectric function and current charges. The Powell method was used for energy minimization. All the co-crystallized ligands and waters were removed, and the random hydrogen atoms were added. The 3D structures of all compounds were constructed by using the sketch molecular modules. Hydrogen and Gasteiger–Hückel charges were assigned to each compound. Then, their geometries were optimized by the conjugate gradient method in TRIPOS force field. The energy convergence criterion is 0.001 kcal/mol. Default values were chosen to finish this work when the protomol was generated. The analysis of intermolecular interactions was performed using Accelrys Discovery Studio 2.5 (Accelrys Software Inc., San Diego, CA, USA).

Results and Discussion

Chemistry

Preparation of the target compounds is shown in Scheme 1. According to the procedures reported previously (9), esterification of acids **2a**–**2g** with propargyl bromide afforded alkyne-functionalized intermediates **3a**–**3g** for further click coupling. Reaction of **OA** with BnCl in the presence of K_2CO_3 in DMF gave benzyl ester **4** in high yield. Then, **4** reacted with 2-chloroethyl chloroformate to afford the chloroacetyl ester **5**. The ester **5** was treated with NaN_3 in the presence of K_2CO_3 in anhydrous DMF at 75 °C for 2 h to give azide **6**. Click chemistry cycloaddition between the azide **6** and corresponding alkyne intermediates **3a**–**3g** was carried out at room temperature in aqueous condition in the presence of catalytic sodium ascorbate and $CuSO_4{\cdot}5H_2O$ to produce triazoles **7a**–**7g** in 83–91% yields. Hydrogenolysis of the triazoles **7a**–**7g** over Pd-C (10%) in THF-MeOH at room temperature gave triterpene acids **8a**–**8g**. The synthesis of proposed structures was found in conformity with spectral analysis.

Biological studies

Glycogen phosphorylase inhibitory activity

The novel compounds described above were evaluated in an enzyme inhibition assay against rabbit muscle glycogen

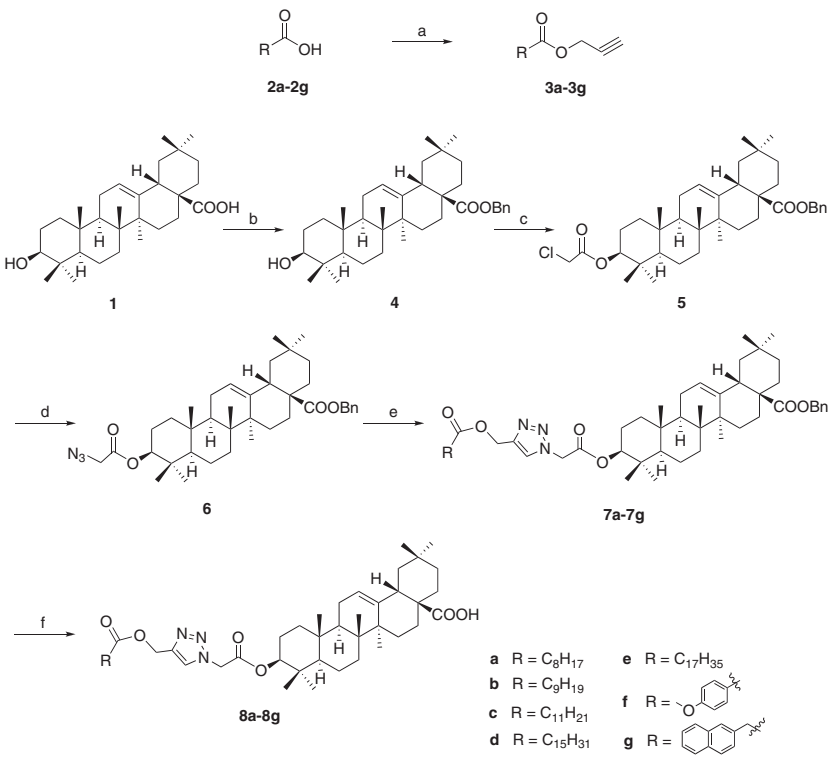

Scheme 1: The synthesis of **OA** derivatives (**8a**–**8g**). (a) Propargyl bromide, K_2CO_3, DMF, r.t. (b) K_2CO_3, BnCl, DMF, 100 °C. (c) $ClCH_2COCl$, K_2CO_3, DMAP, CH_2Cl_2, 0 °C to r.t. (d) NaN3, DMF, 75 °C. (e) **3a**-**3g**, $CuSO_4$·5H2O, sodium ascorbate, CH_2Cl_2-H_2O, r.t. (f) H_2, Pd/C (10%), THF, r.t.

phosphorylase a (RMGPa), an enzyme that shares considerable sequence similarity with human liver GPa. As described previously, the activity of RMGPa was measured through detecting the release of phosphate from glucose-1-phosphate in the direction of glycogen synthesis (11). Caffeine, a known allosteric GP inhibitor that shares the same binding site with **OA**, was used as a positive control (13).

The assay results showed that most of the synthesized compounds exhibited moderate-to-good inhibitory activities against RMGPa (Table 1). The SAR analysis showed that the introduction of an aromatic group led to an increased inhibitory activity. Among the compounds with fatty moieties (**7a**–**7e**, **8a**–**8e**), optimal GPa inhibition activity was observed with the derivative **7c** composed of 12-carbon fatty acid. Predictive SAR was difficult to discern in this case, such as the good potency observed with **7c**, but the lower potency observed with closely related compounds (*e.g.*, **7a**, **7b**, **7d**, **7e**, **8a**, **8b**, **8d**, and **8e**). Among the compounds with aromatic moieties (9), introduction of benzene or substituted benzene ring (*e.g.*, **7f**, and **8f**) resulted in a great loss of activity, while the introduction of naphthalene moiety (**8g**) enhanced the GP inhibitory activity. However, a clear preference could not be established due to the insufficient number of compounds. In this study, SAR analysis of 28-carboxyl group showed that the 28-*O*-benzyl esters are less potent than the corresponding carboxylic acids (*e.g.*, **7a** versus **8a**; **7b** versus **8b**; **7d** versus **8d**; **7e** versus **8e**; **7f** versus **8f**; **7g** versus **8g**) with the exception of derivative **7c**.

Among all these compounds, **8g** is the most potent GP inhibitor with an IC_{50} value of 5.4 μM, stronger than the parent **OA** (IC_{50} = 14 μM).

Glucose consumption in HepG2 cells

HepG2 cell line is a common vitro model to study anti-hyperglycemic agents. It maintains the morphology and function of live cell and is valuable for investigating the liver glucose metabolism (14). To evaluate the effects of synthesized compounds on hepatic glucose consumption, we treated HepG2 cells with different doses of syn-

Table 1: IC_{50} values (μM) for RMGPa inhibition assay results

Compound	RMGPa IC_{50}[a] (μM)	Compound	RMGPa IC_{50} (μM)
1(OA)	14	**7g**	23.9
4	461.0	**8a**	77.1
5	12.6	**8b**	25.6
6	12.7	**8c**	8.4
7a	80.1	**8d**	221.3
7b	143.9	**8e**	11.2
7c	7.76	**8f**	34.6
7d	NI[b]	**8g**	**5.4**
7e	NI	**Caffeine**[c]	144
7f	38.9		

[a]Each value represents the mean of three determinations.
[b]NI means no inhibition.
[c]Caffeine was used as positive control.
The bold values indicates the best inhibition value with an IC_{50} value of 5.4 μM.

Table 2: Effects of **OA**, **OA** derivatives on glucose consumption in HepG2 cells

Compounds	1 μM (%)	10 μM (%)
Negative control, NC, 0.1% DMSO	1.68 ± 0.70	
OA	9.96 ± 1.31**	17.02 ± 1.56***
8a	27.11 ± 4.34***	35.23 ± 2.94***
8b	13.88 ± 2.89**	19.77 ± 1.15***
8c	16.05 ± 4.21***	25.12 ± 2.24***
8d	16.27 ± 4.74***	24.28 ± 1.54***
8e	20.23 ± 5.66***	31.74 ± 3.23***
8f	9.37 ± 2.73**	17.91 ± 0.71***
8g	**23.96 ± 5.20*****	**33.21 ± 1.95*****
Positive control, PC, 0.1 μM Insulin	9.45 ± 1.72**	

Values are mean ± SD; $n = 6$ in each condition. Incubation time: 24 h. The glucose concentration of medium: 11.11 mM.
**$p < 0.01$ for comparisons against the negative control group (0.1% DMSO).
***$p < 0.001$ for comparisons against the negative control group (0.1% DMSO).
The bold values indicates the best inhibition value with an IC_{50} value of 5.4 μM.

thesized compounds and measured the glucose consumption by glucose oxidase method. The assay results (Table 2) show that most of the newly synthesized compounds exhibited strong activities in the stimulation of glucose consumption *in vitro*. The glucose consumption enhancement was notably in a dose-dependent manner. Moreover, SAR analysis suggests that the introduction of bulky groups at C-3 position increased the glucose consumption activity except for compound **8f (e.g.**, **8a**, **8b**, **8c**, **8d**, **8e**, **8g)**. Furthermore, it is implied that the substituents surrounding C-3 might prefer to fatty moieties as evidenced by that good potency was observed with compounds **8a**–**8e**. Within these compounds, compound **8a** exhibited the best activity, a 20.9-fold increase observed at the concentration of 10 μM compared with untreated cells. As shown in Figure 2, compounds **8a**, **8c**, **8d**, **8e**, **8g** (each at 1 and 10 μM) and positive reference insulin (at 0.1 μM) induced a significant increase in the consumption of extracellular glucose compared to the blank vehicle 0.1% DMSO ($p < 0.01$). However, the former analysis on glycogen phosphorylase shows that compound **8g** displayed the best inhibition against RMGPa. Taken together, compound **8g** exerted both good GP inhibitory activity ($IC_{50} = 5.4$ μM) and good activity of glucose consumption enhancement. These results should be helpful to the further modification of OA and thus benefit the potential use of **OA** in the treatment for hyperglycemia. To further identify the proteins responsible for the glucose consumption activity of these compounds, we have carried out a search. The findings will be reported in due course.

Docking study

To explore the binding mode of the synthesized compounds with GP, the most potent compound **8g** was selected for subsequent molecular docking simulation. The crystal structure of GP complexed with maslinic acid (PDB code: 2QN2) was used in the molecular docking simulation. Compound **8g** was predicted to bind at the allosteric site exclusively as shown in Figure 3. This complex was structurally refined by energy minimization in Sybyl X 2.0. This model showed that the **OA** moiety of compound **8g** occupied the location same as malinic acid at the allosteric site in the crystal structure. The triazole linker and naphthalene ring of compound **8g** extended out into a deep hydrophobic pocket. This might explain why compound **8g** ($IC_{50} = 5.4$ μM) exhibited more potency of GP inhibition than compound **8f** ($IC_{50} = 34.6$ μM). The hydrogen bonding interactions formed between the compound **8g** and the protein are illustrated in Figure 3A. Specifically, the hydroxyl oxygen at C-3 position formed hydrogen bonding interactions with Arg193, while the carboxylate oxygen exploited the allosteric effector

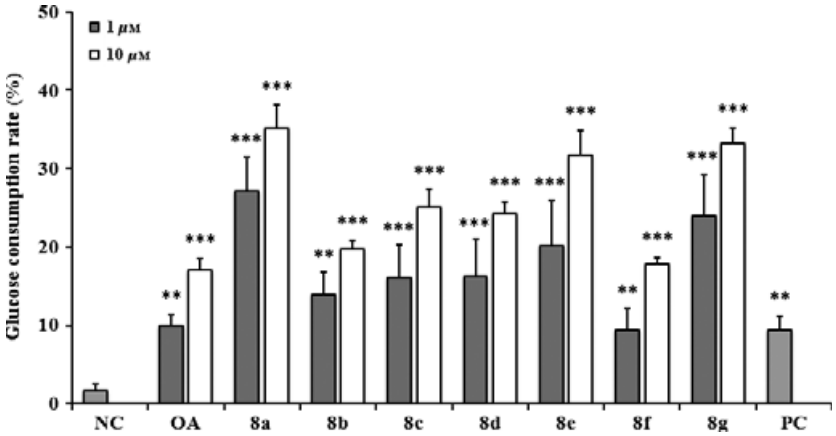

Figure 2: Effects of **OA**, **OA** derivatives (**8a**–**8g**, 1 or 10 μM), and insulin (**PC**, positive control, 0.1 μM) on glucose consumption of HepG2 cells. Mean ± SD; $n = 6$; **$p < 0.01$ and ***$p < 0.001$, for comparisons against the negative control group (0.1% DMSO).

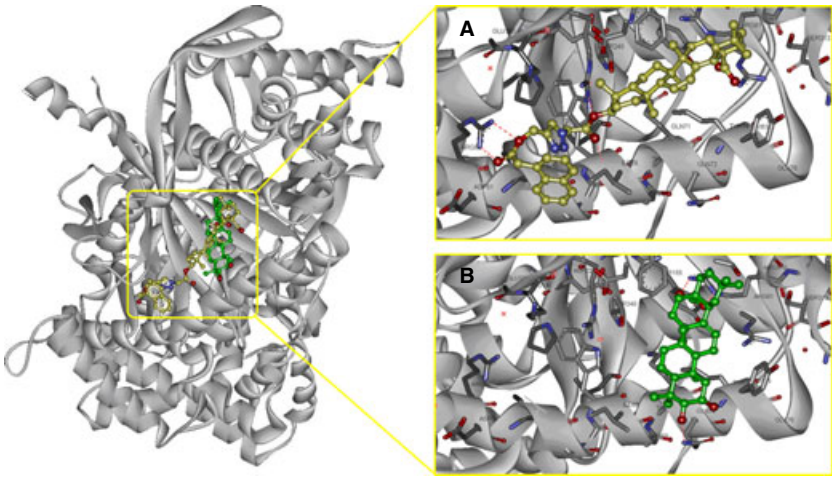

Figure 3: Binding details of glycogen phosphorylase complexed (A) with compound **8g** and (B) with reference compound malinic acid. Residues at the allosteric site are displayed in line style and colored differently. Compounds are represented with ball and stick representation. Hydrogen bonding interactions are shown as red dashed lines. This figure was generated by DS Visualizer 2.5.

phosphate-recognition subsite by forming hydrogen bonding interactions with Arg310. There were additional hydrogen bond formations between the naphthalene ester carboxylate oxygens and Arg60. These two hydrogen bonds may account for the significant increase in GP inhibitory activity of **8g** compared with reference compound malinic acid (IC_{50} = 28 μM) (8).

Conclusion and Future Directions

In summary, we have described the development of a series of oleanolic acid derivatives that can inhibit hepatic glucose production and stimulate hepatic glucose consumption at the same time. The synthesized compounds were evaluated biologically as inhibitors of glycogen phosphorylase, an enzyme that related to high hepatic glucose production. The results showed that most of the newly synthesized compounds exhibited a significant inhibitory activity against rabbit muscle glycogen phosphorylase a (RMGPa). Moreover, they could significantly enhance glucose consumption in HepG2 cells. Compound **8g** exhibited the best activity in inhibiting glycogen phosphorylase and satisfactory activity in promoting glucose consumption. The possible binding mode of compound **8g** with glycogen phosphorylase was also explored. All these data suggested that **8g** was a potential agent for glucose disorders, and further, the development of this compound may be of interest.

Acknowledgments

The work was supported by the National Natural Science Foundation of China (No. 81001401 and 21002125), the Natural Science Foundation of Hebei Province, China (No. H2012406011), and the Science Foundation for Excellent Youth Scholars of Education Department of Hebei Province, China (No. Y2012026).

References

1. Konig M., Bulik S., Holzhutter H.G. (2012) Quantifying the contribution of the liver to glucose homeostasis: a detailed kinetic model of human hepatic glucose metabolism. PLoS Comput Biol;8:e1002577.
2. Lebovitz H.E. (2011) Insulin: potential negative consequences of early routine use in patients with type 2 diabetes. Diabetes Care;2:S225–S230.
3. Hancock A.S., Du A., Liu J., Miller M., May C.L. (2010) Glucagon deficiency reduces hepatic glucose production and improves glucose tolerance in adult mice. Mol Endocrinol;24:1605–1614.
4. Wu C., Okar D.A., Kang J., Lange A.J. (2005) Reduction of hepatic glucose production as a therapeutic target in the treatment of diabetes. Curr Drug Tergets Immune Endocr Metabol Disord;5:51–59.
5. Gao D.W., Li Q.W., Li Y., Liu Z.H., Liu Z.W., Fan Y.S., Han Z.S., Li J., Li K. (2007) Antidiabetic potential of oleanolic acid from Ligustrum lucidum Ait. Can J Physiol Pharm;85:1076–1083.
6. Sung H.Y., Kang S.W., Kim J.L., Li J., Lee E.S., Gong J.H., Han S.J., Kang Y.H. (2010) Oleanolic acid reduces markers of differentiation in 3T3-L1 adipocytes. Nutr Res;30:831–839.
7. Sheng H.M., Sun H.B. (2011) Synthesis, biology and clinical significance of pentacyclic triterpenes: a multi-target approach to prevention and treatment of metabolic and vascular diseases. Nat Prod Rep;28:543–593.
8. Wen X.A., Sun H.B., Liu J., Cheng K.G., Zhang P., Zhang L.Y., Hao J., Ni P.Z., Zographos S.E., Leonidas D.D., Alexacou K.M., Gimisis T., Hayes J.M.,

Oikonomakos N.G. (2008) Naturally occurring pentacyclic triterpenes as inhibitors of glycogen phosphorylase: synthesis, structure-activity relationships, and X-ray crystallographic studies. J Med Chem;51:3540–3554.
9. Liang Z.J., Zhang L.Y., Li L.C., Liu J., Li H.L., Zhang L.Y., Chen L.M. *et al.* (2011) Identification of pentacyclic triterpenes derivatives as potent inhibitors against glycogen phosphorylase based on 3D-QSAR studies. Eur J Med Chem;46:2011–2021.
10. Kolb H.C., Sharpless K.B. (2003) The growing impact of click chemistry on drug discovery. Drug Discov Today;8:1128–1137.
11. Martin W.H., Hoover D.J., Armento S.J., Stock I.A., McPherson R.K., Danley D.E., Stevenson R.W., Barrett E.J., Treadway J.L. (1998) Discovery of a human liver glycogen phosphorylase inhibitor that lowers blood glucose *in vivo*. Proc Natl Acad Sci;95:1776–1781.
12. Wu H.S., Yu J.H., Li Y.Y., Yang Y.S., He Q.J., Lou Y.J., Ji R.Y. (2007) Insulin-sensitizing effects of a novel alpha-methyl-alpha-phenoxylpropionate derivative *in vitro*. Acta Pharmacol Slin;28:417–422.
13. Ekstrom J.L., Pauly T.A., Carty M.D., Soeller W.C., Culp J., Danley D.E., Hoover D.J., Treadway J.L., Gibbs E.M., Fletterick R.J., Day Y.S., Myszka D.G., Rath V.L. (2002) Structure-activity analysis of the purine binding site of human liver glycogen phosphorylase. Chem Biol;9:915–924.
14. Chandrasekaran K., Swaminathan K., Chatterjee S., Dey A. (2010) Apoptosis in HepG2 cells exposed to high glucose. Toxicol In Vitro;24:387–396.